Critical slowing down at a bifurcation

J. R. Tredicce and G. L. Lippi[a)]
Institut Non Linéaire de Nice, UMR 6618 CNRS–UNSA, 1361 Route des Lucioles, F-06560 Valbonne, France

Paul Mandel
Optique Nonlinéaire Théorique, Campus Plaine CP 231, Université Libre de Bruxelles, 1050 Bruxelles, Belgium

B. Charasse,[b)] A. Chevalier,[b)] and B. Picqué[b)]
Département de Physique, Université de Nice-Sophia Antipolis, Parc Valrose, F-06108 Nice, Cedex, France

(Received 10 June 2002; accepted 2 February 2004)

Critical slowing down near a bifurcation or limit point leads to a dynamical hysteresis that cannot be avoided by sweeping a control parameter slowly through the critical point. This paper analytically illustrates, with the help of a simple model, the bifurcation shift. We describe an inexpensive experiment using a semiconductor laser where this phenomenon occurs near the threshold of a semiconductor laser. © *2004 American Association of Physics Teachers.*
[DOI: 10.1119/1.1688783]

I. INTRODUCTION

The study of bifurcations has gained considerable attention in recent decades due to the role that they play in the characterization of the behavior of nonlinear systems. The transition from one state to another is accompanied by the exchange of stability (or at least by a modification of the basin of attraction) of coexisting solutions. Such a change of state can in many instances be characterized by simple, generic equations, whose topological properties closely describe the system's states and the transitions between them. Bifurcations are reported in varied nonlinear systems, from mechanical systems[1] (for example, magnetostrictive ribbons, a spinning top, and a bouncing ball), to spin waves in ferromagnetic materials,[2] chemical[3] and hydrodynamical systems,[4] and lasers.[5] A good introduction to bifurcations can be found in Ref. 6.

In this paper we highlight a counterintuitive property of bifurcations. Suppose that by varying a control parameter μ such as the temperature, a driving electric current, or a chemical concentration, we find a phase transition such that one phase is stable if $\mu<\mu_c$ and the other phase is stable if $\mu>\mu_c$. This behavior is static, obtained by choosing a value of μ, letting the system relax to its final state, and repeating the procedure for each value of μ. However, it often is practical or even necessary to vary the control parameter continuously in time. Such a change is especially true if a large amount of data has to be accumulated to perform a statistical analysis. The counterintuitive result is that if the control parameter is varied from $\mu<\mu_c$ to $\mu>\mu_c$, the bifurcation point is shifted from μ_c, no matter how slowly μ is varied. This topic has been the subject of numerous investigations devoted to studying the general properties,[7,8] or the specific characteristics of a system,[9] or to exploiting the bifurcation's features for particular applications[10] (for example, the removal of chaotic states and the stabilization of particular orbits). Given the generality of the phenomenon, its far-reaching consequences, and that common intuition suggests the wrong answer, it is worth looking at it in some detail. The fact that a simple and inexpensive experiment can be conducted by students in a junior or senior year lab makes the choice of including it in the undergraduate curriculum compelling.

The purpose of this paper is to present this experiment to introduce the students to delayed (or dynamical) bifurcations by testing some of their basic properties. We suggest that the students first be given the setup and be asked to do the experiment, without previous knowledge of the theory behind it. They will be quite puzzled by the result and be highly receptive when the explanation for the phenomenon is presented in the simple terms we use in this paper. We have chosen to keep the presentation as simple as possible. The instructor can complement our presentation with additional material, including a more rigorous approach to the problem if the students possess adequate background knowledge.

Section II presents the general conceptual framework of the problem, which is developed analytically in a straightforward, but sufficiently complete way in Sec. III. Section IV discusses the experiment using a simple and inexpensive optical setup, and compares the experimental results to the analytical predictions. Some general comments are offered in Sec. V, and specific difficulties encountered by the students are addressed in Sec. VI. A set of questions that can be posed to students is given in Sec. VII, followed by our conclusions in Sec. VIII.

II. CONCEPTUAL FRAMEWORK

One of the most common signatures of nonlinear phenomena is the occurrence of coexisting solutions of nonlinear differential equations. This coexistence may take different forms. One common form of coexistence is hysteresis: three solutions coexist, one of which is always unstable, while the other two may have domains of stability and instability. These solutions are connected by limit points. A second form of coexistence occurs in the vicinity of bifurcation points, where two branches of solutions cross and exchange stability.

In both cases, bistability or, more generally, multistability, is linked to a critical point, either a limit point or a bifurcation point. We shall limit our consideration to stationary solutions, although they can be generalized to time-dependent

states. The multiplicity of solutions requires a stability analysis to determine the stability of the different solutions and their basin of attraction. In general, it is not possible to carry through such an ambitious program. In exceptional cases, some simplified models admit exact solutions and a complete stability analysis is then possible (see Sec. 4.4.1 of Ref. 11 for an example). In most cases, one has to resort to a linear (local) stability analysis, testing the stability of a solution against infinitesimal perturbations. This analysis leads to a characteristic equation for the rates at which the perturbation decays (stable solution) or grows (unstable solution). This characteristic rate may be complex, in which case the decay or the growth of the perturbation is modulated at a frequency given by the imaginary part of the rate. By definition, a critical point is a point where the real part of a rate vanishes, a property common to limit points and bifurcation points.

III. ESCAPING CRITICAL SLOWING DOWN

The inverse of the real part of a characteristic rate is a relaxation time. Hence, a critical point is characterized by an infinite relaxation time. The vicinity of a limit point is characterized by critical slowing down. The magnitude of the relaxation time is controlled by the distance from the critical point; as the critical point is approached, the time scale becomes longer, which means that the dynamics of the system is no longer governed by the usual time scales, such as the atomic relaxation time or the cavity photon lifetime in optics. Rather, the response time is determined by the topological structure and the resulting dynamics is universal. The amount of slowing down can be considerable and in optical systems an increase in time scale by up to six orders of magnitude for the relaxation times has been reported.[12]

Critical slowing down often is unwanted. A classic strategy to evade critical slowing down is to sweep the control parameter across the critical point. The rationale behind this procedure is that if the sweep rate is small enough, the dynamical system should quasi-statically follow the stationary state. This line of reasoning holds far away from critical points, but it turns out to be incorrect close to a critical point.

Let us illustrate these ideas with a simple example that contains all the necessary elements. We consider a system that has two steady states (denoted by a tilde), $\tilde{x}=0$ and $\tilde{x}=A$, where A is the control parameter. We assume that the dynamics of the system can be described by

$$\frac{dx}{dt}=x(A-x). \tag{1}$$

The bifurcation point is at $A=0$. The zero solution is stable if $A<0$ and unstable if $A>0$. Conversely, the solution $\tilde{x}=A$ is unstable if $A<0$ and stable if $A>0$. Figure 1 illustrates the stability exchange (solid line: stable solution; dashed line: unstable one). The bifurcation corresponds to the stability exchange between the two solutions, where the change in behavior of the system passes from a state independent of the value of the control parameter A, because for $A<0$ we always have $\tilde{x}=0$, to one that depends explicitly on A.

We are interested in the transition between the two states when A changes in time, beginning with $A<0$ and crossing the point $A=0$. As long as the solution remains in the neighborhood of $x=0$, a local analysis can be performed by expanding Eq. (1) to first order in the neighborhood of $x=0$ (that is, $dx/dt\simeq Ax$). To describe the effect of the sweep, we introduce an explicit time-dependence by setting $A=\mu(t)$, so that Eq. (1) becomes $dx/dt=x(\mu(t)-x)$. Notice that $\tilde{x}=0$ remains an exact solution, independent of the functional time dependence of μ. Therefore, the linearized form holds in general, and the evolution is correctly described by

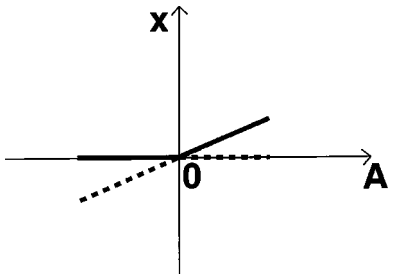

Fig. 1. Steady state solutions of Eq. (1). Stability is denoted by the solid line. The $x=0$ solution is stable for $A<0$, while the $x=A$ solution is stable for $A>0$. The exchange in stability occurs at $A=0$, the (static) bifurcation point.

$$\frac{dx}{dt}=\mu(t)x, \tag{2}$$

as long as the solution $x(t)$ remains close to zero. When this solution is no longer valid, the solution $x(t)$ abandons the neighborhood of zero and diverges exponentially, and the transition to a finite value of $x(t)$ has occurred. In this case, Eq. (2) no longer describes the dynamics, but we can characterize the transition by the time at which the solution $x(t)$ starts increasing away from zero. Hence, the operational definition of a dynamical bifurcation, that is, the occurrence of a bifurcation in a time-dependent regime, will be defined as the deviation from the previous, zero solution.

Equation (2) can be formally integrated to obtain the solution

$$x(t)=x(0)\exp\left[\int_0^t \mu(t')dt'\right]. \tag{3}$$

We call $\bar{t}$ the time at which the parameter $\mu(t)$ reaches the bifurcation point. This value is obviously defined by

$$\mu(\bar{t})=0, \tag{4}$$

which determines the static bifurcation, because at this instant the control parameter is zero. The value of the parameter for which

$$x=0, \quad \mu=0, \tag{5}$$

defines the position of the static bifurcation. At time $\bar{t}$ the control parameter reaches the value for which the linear stability analysis predicts a change in stability for the dynamical system. For $t<\bar{t}$, we have $\mu(t)<0$, and therefore $x(t)=0$.

For a time-dependent system, reaching the condition specified by Eq. (4) does not give rise to a change in physical behavior. Indeed, while in the static problem (the result of the usual linear stability analysis where all parameters are kept constant) the point defined by Eq. (5) corresponds to the exchange of stability, in the swept-parameter case the condition $\mu(\bar{t})=0$ does not. We immediately recognize this fact by observing from Eq. (3) that $x(t)$ starts to diverge away from $x(0)$ only when the argument of the exponential func-

tion goes from negative to positive values. For negative values the perturbation relaxes to zero, and only for positive values can it grow from $\tilde{x}=0$.

We therefore define another quantity: the *dynamical bifurcation* point, a concept that can exist only if the control parameter is time-dependent. It is defined as the time at which the solution $x(t)$ in Eq. (3) begins to diverge:

$$\int_0^{t^*} \mu(t')dt' = 0. \tag{6}$$

Equation (6) is an implicit equation for the time t^* and can be solved once an explicit form for $\mu(t')$ has been specified. When a solution exists, we can infer some of its basic features from some elementary considerations.

We have assumed that $\mu(t)$ is an increasing function of time, because we want to study the transition from the parameter-independent solution ($\tilde{x}=0$) to the other solution. Hence, $\mu(0)<0$. If $\mu(t)$ is monotone (but otherwise generic), we know that until time $\bar{t}$ $\mu(t)\leqslant 0$ for $t<\bar{t}$. Therefore, we are certain that $\int_0^t \mu(t')dt'<0$. As a consequence, at the time the static bifurcation has been reached, the system is still stable on the $\tilde{x}=0$ branch. In order for the solution to be destabilized, the integral between $\bar{t}$ and t^* must "accumulate" the right amount of positive "area" to compensate for the "negative" area that has accumulated between 0 and $\bar{t}$:

$$\int_{\bar{t}}^{t^*} \mu(t')dt' = -\int_0^{\bar{t}} \mu(t')dt' = \left| \int_0^{\bar{t}} \mu(t')dt' \right|. \tag{7}$$

Let us illustrate these considerations with an explicit example, where we assume a linear dependence of the control parameter on time:

$$\mu(t) = -A_0 + vt \quad (v, A_0 > 0). \tag{8}$$

Such a dependence is not only convenient mathematically, but also can be implemented experimentally, as discussed in Sec. IV. The integration of Eq. (3) is immediate using Eq. (8), and the conditions given in Eqs. (5) and (6) become:

$$-A_0 + v\bar{t} = 0, \tag{9}$$

$$-A_0 t^* + \frac{v}{2} t^{*2} = 0. \tag{10}$$

From Eqs. (9) and (10) we obtain

$$t^* = 2\bar{t}, \tag{11}$$

$$\mu(t^*) = -\mu(0), \tag{12}$$

and thus the time at which the dynamical bifurcation occurs is twice the time necessary for reaching the static bifurcation, independent of the speed at which the parameter is swept! This result appears to be completely counterintuitive, because one might expect that the sweeping speed v should play a role in the position of the dynamical bifurcation.

A graphical illustration of the results provided by Eqs. (11) and (12) is given in Fig. 2. We see that the area under the triangle in the $\mu<0$ half plane has to be equal to that in the $\mu>0$ half plane [because of Eqs. (6) and (7)]. Because, for ease of illustration (and experimental realization), we have chosen a linear dependence for the parameter, $\mu(t)$, the two triangles of Fig. 2 are equal, and therefore the time necessary

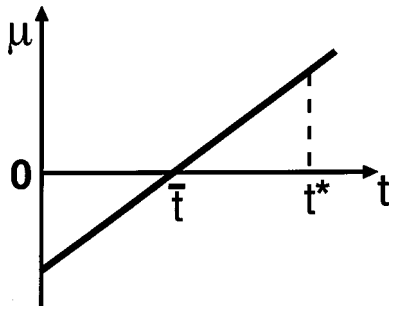

Fig. 2. Illustration of the principle expressed by Eq. (7). The negative area accumulated in the triangle below the t axis (that is, between $t=0$ and $t=\bar{t}$) has to be equal to the positive area accumulated between $t=\bar{t}$ and $t=t^*$ to attain the dynamical bifurcation point.

to reach the dynamical bifurcation is double that of the static one, Eq. (11), independent of the speed v. This condition is a direct consequence of the fact that for the areas to be equal, the value of μ for which the dynamical bifurcation is reached, $\mu(t^*)$, must be equal in absolute value to the initial value of μ, $\mu(0)$.

Another very important point resulting from the analysis is that the time required to reach the static bifurcation $\bar{t}$ (thus also t^*) depends inversely on the sweep rate: $\bar{t}=a_0/v$ (where $A_0>0$ is the initial μ value). Hence, if the sweep is conducted at a slow rate, the time necessary to reach both static and dynamic bifurcation will be correspondingly longer. Although obvious, on the basis of the mathematical derivation, the results provided by Eqs. (8)–(12) are entirely counterintuitive. Indeed, the limit in which the bifurcation is scanned with vanishingly small values of the sweep rate ($v \to 0$) yields a completely different result from the static bifurcation. In the dynamical case the time for reaching the bifurcation diverges ($\bar{t}, t^* \to \infty$), and hence the control parameter value for which it occurs is (mathematically) shifted to infinity. Instead, in the static case the control parameter is kept constant and therefore the position of the bifurcation in parameter space is fixed at its equilibrium value.

What happens in the dynamical case is that there is an accumulation of stability (the integral between 0 and $\bar{t}$), which has to be compensated by going beyond the bifurcation for a certain time. Slowing down the scan only increases the time necessary to achieve the necessary compensation.

Note that the time at which the system loses stability also depends on the initial condition A_0. The larger the magnitude of $|A_0|$, the longer are $\bar{t}$ and t^*, because the system needs more time to reach the static bifurcation and thus has accumulated a greater amount of stability. Therefore, the system can follow the statically unstable solution for a longer time, as illustrated qualitatively in Fig. 3, where the solid line represents the actual trajectory $x(t)$, and as confirmed by the experimental results of Sec. IV [see in particular, Fig. 6(b)]. A comparison of Figs. 3 and 1 shows that the solution has remained on the $x=0$ branch for a longer time than predicted by a static linear stability analysis.

In summary, we see that the limit of the static bifurcation can be approached only by keeping the ratio A_0/v as small as possible. This limit is obtained either by starting the system infinitely close to the threshold (but fluctuations, which are not included in this treatment, will become important, see

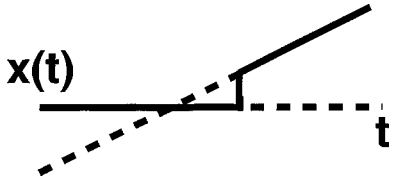

Fig. 3. Dependence of x as a function of the time t when the bifurcation is swept (for increasing values of μ). The static bifurcation point (crossing of the solutions) is passed with $x(t)$ remaining on the unstable solution for some time, before jumping toward the new stable solution. In the opposite sweep x remains on the other solution for a while in spite of its being unstable.

Sec. V), or by using a very large sweep speed, ideally $v \to \infty$. Hence, contrary to intuition, the static bifurcation is approached in the limit in which the system is swept across the bifurcation at infinite speed.

We remark that the long-dashed line in Fig. 3, which illustrates the evolution of $x(t)$ beyond the bounds of validity of our local analysis, is nothing but an educated guess about what $x(t)$ will do after abandoning the $\tilde{x}=0$ branch. Indeed, because only one other solution is available, $\tilde{x}=A$, and because this solution is stable, it is plausible that the system will converge toward it and that it will do so asymptotically. In Sec. V we will comment on a small difference between this prediction and the experimental situation.

IV. EXPERIMENT

The experimental apparatus is shown in Fig. 4. The output power of a semiconductor laser[13] driven by a modulated/variable power circuit is focused on a solid state detector.[14] The current supplied to the laser is controlled by a standard signal generator. The detector and signal generator outputs are observed with a two-channel digital oscilloscope. The oscilloscope is interfaced to a personal computer to analyze the data. The laser operates in the red region of the optical spectrum ($\lambda \approx 670$ nm, maximum power ≈ 4.2 mW).[15]

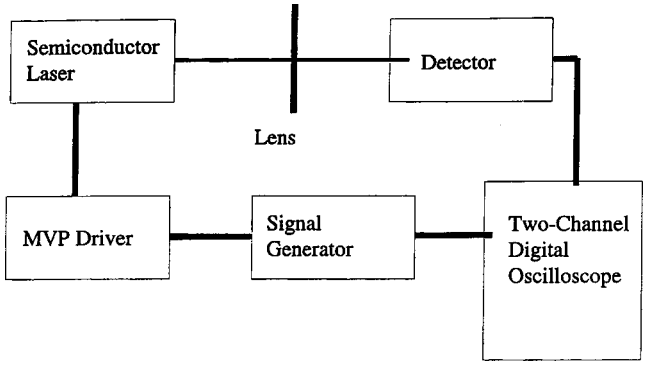

Fig. 4. Schematics of the apparatus. The laser output (see Ref. 13) is focused through a standard lens onto a Si PIN detector (see Ref. 14), connected to a digital oscilloscope (HP54602B digital oscilloscope, 150 MHz, with a HP54657A Measurement/Storage Module HP-IB interface) through a 50 Ω adaptor. The signal from the function generator is simultaneously recorded by the oscilloscope on a second trace. A function generator (Tektronix CFG253, 3 MHz bandwidth) drives the laser through its stabilized power supply (modulated/variable power circuit driver by Thorlabs), which includes protection against junction bias reversal and overvoltage; without input signal, this driver supplies the laser to obtain about 90% of its maximum power.

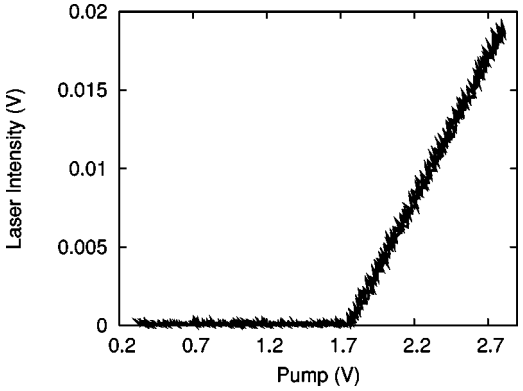

Fig. 5. Laser intensity as a function of pump voltage (signal level from the function generator). The pump voltage changes from 0.3 to 2.8 V. The laser threshold appears for $V=V_{th}=1.78$ V. In this figure and Fig. 6 we plot the data in a way which resembles the oscilloscope's output.

Initially, we determine the threshold voltage and the laser intensity as a function of the pump, that is, the amount of current flowing through the semiconductor junction, injected by the power supply (MVP driver by Thorlabs, cf. Fig. 4), and controlled by the voltage level at the output of the signal generator. We set the offset of the signal generator at around $V_{bias}=+1.55$ V and apply a triangular signal at very low frequency (of the order of 5 Hz) and amplitude 2.5 V (peak-to-peak) to control the injection current. The voltage on the semiconductor laser changes from $V_{min}=+0.3$ V to $V_{max}=+2.8$ V. By setting the oscilloscope in the $x-y$ mode, we can directly observe the laser intensity as a function of pumping voltage.

A typical result is shown in Fig. 5. Several conclusions can be drawn by simple inspection: (i) there exists a pumping value $V_{thr}=+1.78$ V below which the output intensity is constant[16] at $I=0$; (ii) the intensity I grows linearly with the pumping voltage for $V>V_{thr}$; and (iii) the transition from the $I=0$ state to the $I\neq 0$ state appears to be continuous, devoid of hysteresis. In addition, there is no sign of critical slowing down, even though there is an exchange of stability between two different branches. We thus could assume that the measurement is done quasi-statically: the system reaches the steady state value before the parameter changes appreciably. In other words, the experiment appears to show that there is no coexistence of states even close to the bifurcation point (the laser threshold). We will now show that this conclusion is erroneous, and that critical slowing down can be seen by modifying the parameters involved in the measurement.

Without changing the experimental apparatus, we just increase the frequency of the triangular voltage signal to 40 kHz, without modifying its amplitude and bias voltage. In Fig. 6 we show a typical trace of (a) the laser intensity and the pumping voltage as a function of time, and (b) the laser intensity as a function of pumping voltage. We observe that for increasing signal level, the laser switches on at a pumping voltage V^* which is higher than the previously measured V_{thr}. At $V=V^*$, the intensity increases suddenly from 0 to the ''large'' value, which corresponds to the above-threshold value of the instantaneous pump. This jump is visible in the lower trace of Fig. 6(a), where the laser intensity suddenly grows from the low level (spontaneous emission) to the triangular shape which follows the current injected in the junc-

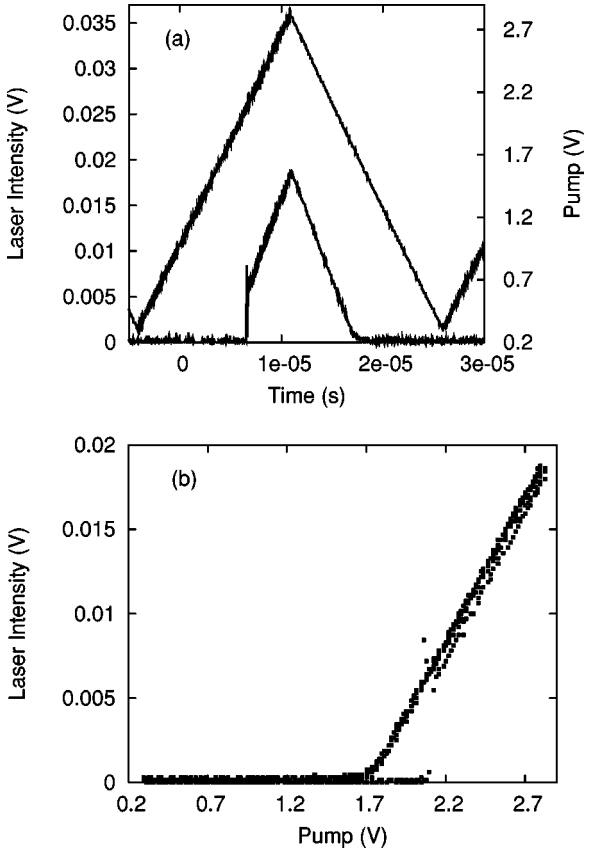

Fig. 6. (a) Laser intensity (bottom trace, left vertical scale) and pump voltage (top trace, right vertical scale) as a function of time for a frequency of the triangle wave applied by the function generator, $f \approx 40$ kHz. In analogy with the notation of Sec. III, V^* represents the voltage value at which the laser switches on (for increasing pump values), while turn-off occurs at $V = V_{\text{th}}$ for decreasing pump. In the notation of Sec. III, V_{th} should be expressed as $\overline{V}$. We prefer using the traditional notation V_{th} which is widely recognized in laser physics. (b) Laser intensity as a function of pump voltage. The graph shows bistability in the interval $V_{\text{th}} \leqslant V \leqslant V^*$. The traces (plotted with points to better highlight the effect) are slightly separated on the diagonal branch (the lower occurs for increasing pump, the higher for decreasing pump) because of the speed at which the laser is driven.

tion. A comparison of Figs. 6(b) and 3 is very instructive: the delayed jump is visible in the experimental trace (plotted with dots—we suggest that the same be done by using the ''dots'' options available on most oscilloscopes). As we decrease the voltage, the laser intensity remains proportional to the pumping voltage until it vanishes at $V = V_{\text{thr}}$. Thus, there is hysteresis for $V_{\text{thr}} < V < V^*$, which can be straightforwardly and clearly displayed using the $x-y$ mode of the oscilloscope [Fig. 6(b)], and shows directly the coexistence of two different states. Notice that there is not a perfect superposition of the traces in the part of the branch where the laser intensity follows the pump [Fig. 6(b)]. This behavior is an artifact of the sweep imposed on the parameter, which prevents the system from being instantaneously at equilibrium: the laser retains a memory of its state at the previous instant, and thus the intensity curve is slightly lower when the pump is being increased and higher when it is being decreased.

Note that the slope of the triangular signal is a direct measurement of the parameter's rate of change and this rate is still orders of magnitude smaller than the smallest relaxation rate of the laser (its relaxation time is in the nanosecond range). Furthermore, the difference $V^* - V_{\text{thr}}$ is a direct measurement of the delay time t^* because the voltage is proportional to time. If we keep the amplitude and voltage bias constant, a change in the frequency amounts to only a change in the sweep rate of the pumping parameter.

The theoretical results described in Sec. III show that the time t^* diverges as the sweep rate vanishes. A measurement of the delay time as a function of frequency for the triangular signal should therefore show such behavior. At the same time, if the dynamics are independent of the laser parameters, we should find a universal scaling law for the time t^* as a function of the slope of the triangular function. This prediction can be verified experimentally by measuring the delay time at different scanning frequencies. To do so we keep the amplitude of the modulation constant and simply change the frequency of the triangular wave. Experimentally, we define the delay time as the time starting from the instant at which the triangular wave is at its lowest point, and ending at the instant at which the laser intensity reaches half of its final height (this value is the point with maximum slope, which can therefore be determined most accurately). The measurement of the delay time can be best made by setting the vertical cursors (intensity) at the correct levels (as specified previously) and then using the horizontal ones (time scale) to measure the delay (the oscilloscope's predefined ''difference'' function will provide the delay time directly).

In Figs. 7(a) and 7(b) we plot t^* as a function of $b = dV/dt$, and $\ln(t^*)$ as a function of $\ln(b)$,[17] for different amplitudes and bias voltages. From the plots we conclude that the delay time increases as we decrease the sweep rate and that it diverges for a vanishing sweep rate. Thus, critical slowing down exists at the bifurcation point. Furthermore, the scaling law is of the type $t^* = Cb^x$, where x is independent of the laser parameters and the constant C depends on the amplitude and bias voltage of the triangular signal. We also remark that the scaling law breaks down for large values of the sweep rate and/or V_{min} relatively close to threshold.

V. COMMENTS

This brief section is devoted to a more detailed discussion of some finer points related to the comparison between the paradigmatic model for a dynamical bifurcation, discussed in Sec. III, and the measurements performed on our system. These points are not apparent in our figures, but will become obvious to anyone repeating the experiment and looking for these effects.

As mentioned in Sec. III, if V_{min} is set close to threshold, the system becomes sensitive to noise. In this case, the scaling exponent that we have derived with the simple model cannot hold (see Sec. VI), because noise has not been taken into account. For this reason we cannot reach the limit $A_0/v \to 0$ by choosing a very small value for A_0. There is another reason that restricts the approximation of $dx/dt = x(\mu - x)$ by $dx/dt = \mu x$ to the domain $x \ll 0$. If x is a small quantity, say ε, then the linearized equation $dx/dt = \mu x$ is balanced only if μ is not small. That is, each member of the equation is proportional to ε. However, if A_0 also is a small quantity, comparable to ε, then the right-hand side μx is proportional to ε^2 for small times while the left-hand side remains proportional to ε. This dependence is inconsistent,

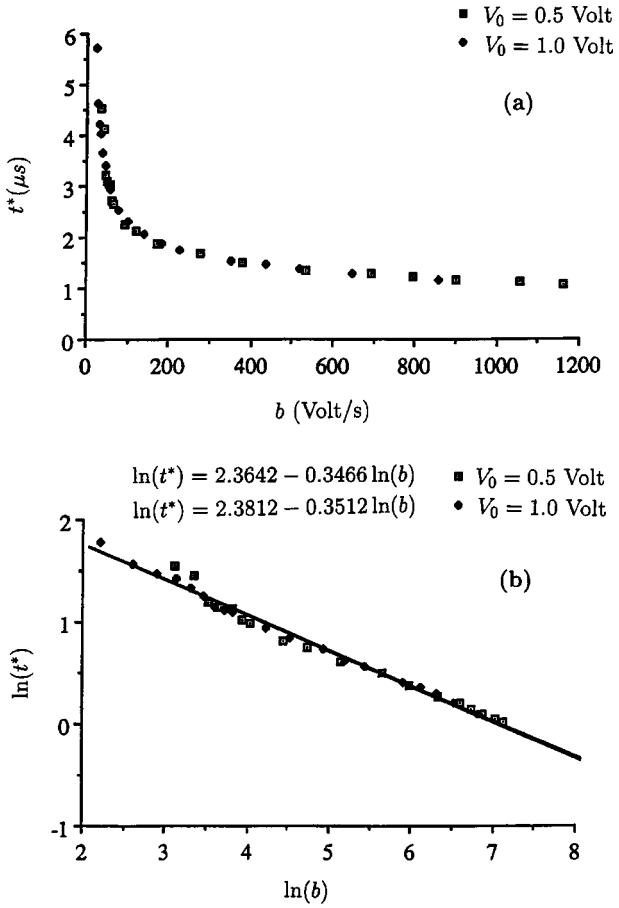

Fig. 7. Scaling law for the time at which the dynamical bifurcation is attained, as a function of the pump voltage slope. (a) The time is plotted as a function of $b=dV/dt$ for two different values of the initial pump (V_0). The data superpose very well, irrespective of the chosen initial condition. (b) Log–log plot (base e) of the previous graph, which allows for the direct determination of the scaling law; the values of the fitted parameters (the straight line is shown to guide the eye) are given in the expression on top of the graph.

and it means that the linearization procedure we have applied to the nonlinear equation $dx/dt=x(\mu-x)$ is no longer valid if both x and A_0 are very small.

The opposite limit, $v\to\infty$, presents experimental difficulties as well. If the values of the sweep rate are very large (for example, obtained by using a square function from the generator, instead of a triangular one), we see that the delay time t^* saturates. This saturation is due to the fact that the experimental system is more properly described by a set of two coupled ordinary differential equations, characterized by different time scales. A discussion of the saturation in the delay time is beyond the scope of this paper, and we refer to Ref. 18 for a physical description of that process. In addition, for the laser in question, the limitation of the electrical bandwidth becomes relevant at high speeds. Because we can correctly describe the behavior at the bifurcation over a range of speeds of about three orders of magnitude, this experiment is a demonstration of the generality of the phenomenon. Even though we described the more complex experimental system with a one-dimensional model, Eq. (1), we still obtained a correct representation of the shifted bifurcation.

The comparison between Figs. 5 and 6 may raise some questions. The hysteresis cycle, visible at high scanning speed (Fig. 6), apparently disappears at low speed (Fig. 5). If true, the disappearance of bistability at low speed would contradict the body of the results that we have discussed (indeed, no bistability loop exists in the static bifurcation). The contradiction is only apparent, as can be easily understood through the following arguments (see Sec. VI for further details). The bistable cycle shrinks and, in theory, never disappears when the scanning speed is reduced. Experimentally, this statement can be verified by adjusting the oscilloscope's scales in such a way as to visualize the cycle at different speeds, until the cycle becomes so small that it disappears into the noise. The shrinking of the cycle comes from the progressively lower speed at which the system advances close to $x=0$ and $\mu>0$ (known as the unstable manifold) after crossing the static bifurcation point. In spite of the increased time delay (see Fig. 7), the speed is slow enough to reduce the total distance covered on the unstable manifold; noise further reduces the portion of unstable manifold followed by the laser (see Sec. VI for further observations on this point). Hence, there is no contradiction between the increase in the time delay and the decrease in the width for the bistable loop for a decrease in the scanning speed. We point out that this feature is characteristic of all dynamically induced hysteresis cycles.

As mentioned in Sec. IV, a careful inspection of the oscilloscope trace in Fig. 6(b) shows that the transition from the lower to the upper branch is accompanied by a (small) overshoot which relaxes on the upper branch with oscillations.[21] This overshoot is an indication of the fact that the dimensionality of our experimental system is larger than that of the model we used to discuss the delayed bifurcation ($D=1$), because oscillations require a minimum dimensionality, $D_{\min}=2$ to occur.[6] Even though there are small deviations that can be highlighted by careful experimental observations, the one-dimensional description of the shifted bifurcation remains an excellent description of the main features observed in most two-dimensional systems.

VI. METHODOLOGICAL DIFFICULTIES

Students have trouble realizing that only the time t^* is experimentally accessible and that their efforts are best spent if they concentrate on it. In addition, the correct measurement of t^* requires care in the use of the oscilloscope—a point that does not always occur to them. The first snag comes from keeping the whole signal on the screen, a natural temptation, but one that renders the measurement inaccurate at low scanning speeds (for lack of time resolution). To compound the problem, this kind of visualization gives the impression that the delay time is reduced at low speeds, because the width of the dynamical hysteresis loop shrinks. This difficulty is easily recognized by comparing Figs. 5 and 6(b), which have been taken at 5 Hz and 40 kHz, respectively. Hence, the students' first reaction is that the functional dependence on speed predicted in Sec. III is incorrect (or, if they haven't yet been presented the theory, they will convince themselves of the validity of the incorrect intuitive image discussed at the beginning of Sec. III).[22] The correct measurement requires plotting the delay time as a function of the input signal's slope, as in Fig. 7. The measurement of t^* is best obtained with the help of the cursors of a digital oscilloscope and the delay features of the trigger so that a sufficiently fine time scale is used to maintain a good level of accuracy throughout the series of measurements.[23] The zero

for time is taken at the beginning of the ramp, a concept that has to be sometimes stressed, together with the fact that different series of measurements starting from different values of the initial current (voltage offset) provide information about the independence (or lack thereof) of the phenomenon on the distance from the critical point (see Fig. 7).

An objection raised by some students is that, *a posteriori*, it is obvious that the delay time should be longer for slower scanning rates, because the time that the system takes to arrive at the bifurcation, starting from the same initial condition, is longer. This objection is clearly valid, but the apparent triviality of the statement hides a subtle point on which all of our considerations depend. The objection holds when thinking about $\bar{t}$, but does not say anything about t^* which, in the absence of a dynamically delayed bifurcation, could approach $\bar{t}$ in the slow scan. The latter conclusion is exactly what (the wrong) intuition would suggest.

We can instead demonstrate that t^* does not approach $\bar{t}$ in a slow scan with the following argument. We do not have an independent measure of $\bar{t}$ to show that t^* satisfies the conditions shown in Sec. III, but it is obvious [see, for example, Fig. 6(b)] that during a fast scan the system changes state well after the static threshold. Hence, we are sure that at high scanning speed there is a dynamical shift of the bifurcation. The graphs of Fig. 7(b) show that the delayed bifurcation crossing also holds for a slow scan, because the scaling is found even at slow speed; this result remains true (with an accuracy of a few percent in the parameters calculated with a standard regression algorithm) for different initial values for the scan. Therefore, the shift that we measure is not simply due to the fact that the slower scans require a longer time to reach the static threshold: the linearity of the point distribution in Fig. 7(b) shows that t^* increases with an inverse power of the speed, that is, the amount of time $(t^*-\bar{t})$ the system spends following the unstable solution also increases in the same way. The graphs and this careful analysis of the results prove the nontriviality of the result.

A more direct way of visualizing the previous considerations can be obtained in the following way, although we stress that even though a visual tool is very helpful, one should not attach too much importance to it. Figure 8 shows a series of measurements performed for different values of the triangle wave frequency and fixed amplitudes. For these measurements, the oscilloscope trigger has been set very close to the static bifurcation value (within $\approx 1\%$). This choice gives the best visualization of the delay, but is not appropriate for quantitative measurements, because the initial time is not correctly defined in this way. The left column shows the initial portion of the period of modulation where the laser emits light, and we can easily recognize the (apparently) increasing part of the modulation where bistability is present. The right column shows the corresponding bistable loops obtained by plotting the laser intensity as a function of the injected current. The latter clearly shows a reduction in the width of the bistable loop when the driving frequency is reduced. This result is in agreement with the visual conclusion that one could draw from the left-hand figures in Fig. 8 and would appear to support the (incorrect) intuitive conclusion that the delay time is reduced when the frequency is lowered. We show this figure and stress the discussion of this point because it is exactly what students conclude from their observations. Many students will use these figures to argue that the slow modulation regime approaches the static bifurcation.

A closer look at the left-hand figures in Fig. 8 shows, however, that this conclusion is a visual trick. If one measures the delay time, rather than simply looking at the shape of the laser intensity, one realizes that it increases for decreasing driving frequency. This delay time is exactly the quantity measured in Fig. 7. An easier way of convincing oneself that the ''shrinking'' bistability loops of Fig. 8 (left) push the experimenter toward the wrong conclusion is to plot multiple switch-on traces on the same scale (see Fig. 9). We see that the time is truly increasing for slower driving: the experimental traces obtained for different frequencies are plotted on two separate panels for better visualization (both time scales and intensity values differ too much for a single graph). The straight lines are plotted to guide the eye and qualitatively extend backward the functional dependence that the laser intensity would have if the delay at the bifurcation did not exist. We remark that (1) all straight lines cross in (approximately) the same point (as can be seen by comparing the absolute scales in the two panels of Fig. 9); (2) the switch-on time is further reduced with increasing driving frequency; (3) the laser follows a larger portion of the unstable manifold at larger driving frequencies (which causes confusion between the increasing width of the bistable loop and the actual reduction of the time delay); and (4) the laser intensity jumps to higher intensity values when the time delay is shorter (and the overshoot is larger). Notice that the crossing point of the straight lines corresponds to the instant at which the swept current encounters the threshold, that is, it occurs when the traces are triggered by the oscilloscope. The fact that the value of the laser intensity is not zero at this time is a finer point which cannot be discussed here and whose origin is related to the nature of class B lasers.[24,25] The longer delay at the bifurcation is now evident, and the corresponding jump toward higher intensity values is obvious, while the larger overshoot is again a feature connected to the larger dimensionality (two) of the phase space representing this laser.[19]

We stress that the curves in Fig. 9 are drawn by taking a portion of the data of Fig. 8 (left). Due to the longer time scales of the slower scans and to the fixed (and limited) number of points that the oscilloscope allows, the rendition of the details becomes poorer [especially for the curves of Fig. 9(a)].

Finally, we remark that the predicted and observed exponents are not the same (see Sec. III and Fig. 7). This discrepancy is a point that bothers those students who believe that no disagreement is to be expected in science. We believe that this conflict between theory and experiment offers the instructor an excellent opportunity to remark on the scope of models and on the limitations of the validity of their predictions. A simple model is preferable to a very complex one, but one must be aware of its limitations and use it only as far as appropriate.

However, we can offer some comments that help in understanding the origin of the discrepancy. First of all, we would expect the difference in the exponent to be related to the complexity of the semiconductor laser, normally described by two coupled differential equations,[26] although the model that we discuss is limited to one dimension. Although the different phase space dimensionality is a limitation of the comparison, it turns out not to be the most important one,

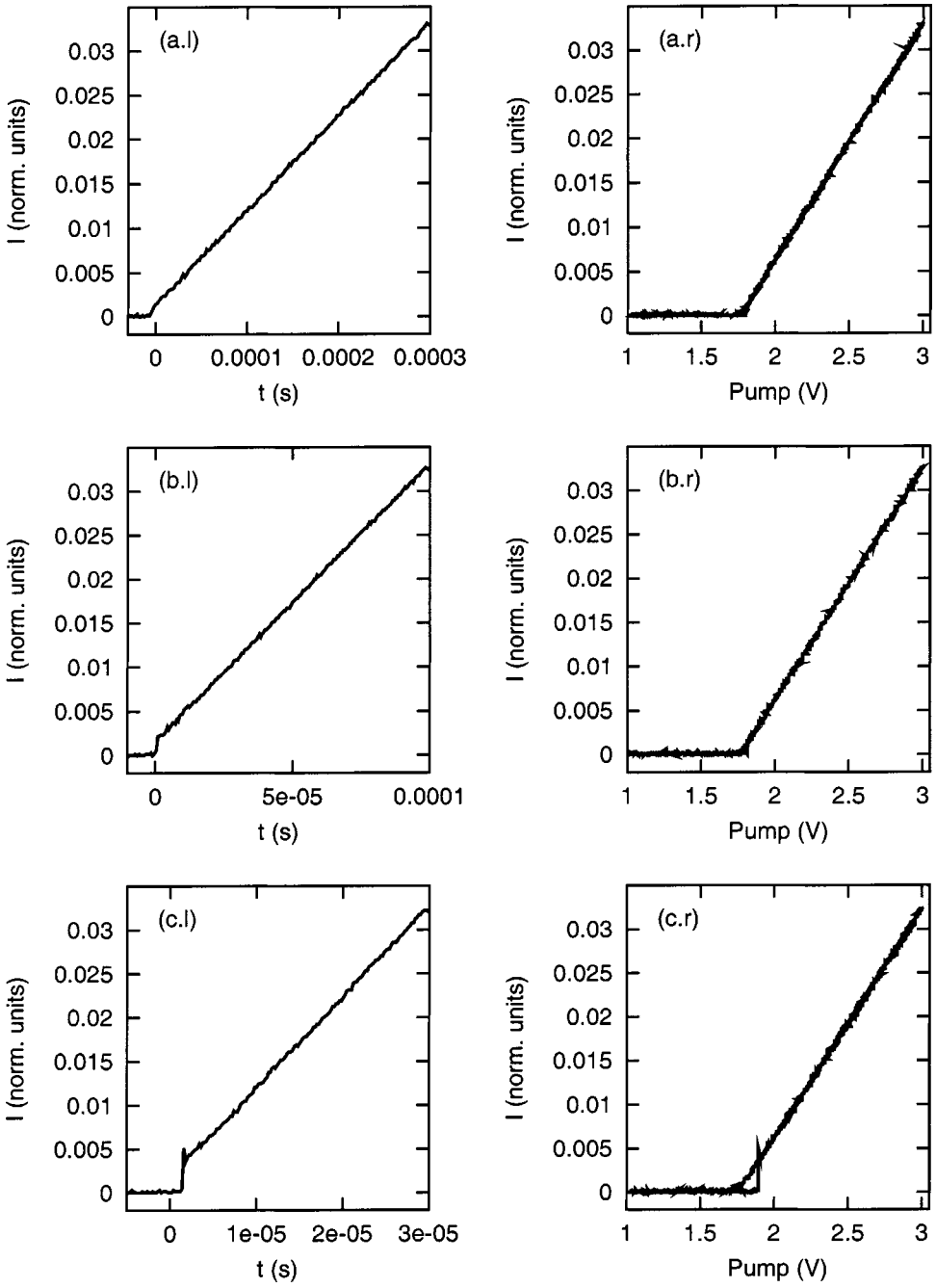

Fig. 8. Details of the upward-scanned laser intensity near threshold for different values of the triangle-wave frequency and fixed amplitude (minimal value of the triangle $V_{min}=1.0$ V, maximal value $V_{max}=3.0$ V). The left-hand column shows the temporal intensity behavior, the right-hand the corresponding laser-intensity vs pump. The bistability loops are well visible in Figs. c.r-f.r (and can be guessed in Fig. b.r). Frequency values of the driving signal: (a) $f=1$ kHz, (b) $f=3$ kHz, (c) $f=10$ kHz, (d) $f=20$ kHz, (e) $f=50$ kHz, (f) $f=80$ kHz. The oscilloscope's trigger is set very close to threshold (within 1%) for best visualization.

because the exponent x differs from -1 even for lasers whose dynamics can be correctly described as one-dimensional.[27]

One cause of the discrepancy, which alert students may notice, is in the different definitions of the delay time used in the theoretical discussion and in the experiment. In Sec. III t^* is defined as the time at which the solution begins to diverge [see Eq. (6)]. Because such a time cannot be measured experimentally due to the smallness of the intensity values compounded by the presence of the intrinsic noise (both the laser's and the electronics used for the measurements), we are forced in the experiment to introduce a different definition. The most convenient is the one used in Sec. IV, because it provides the best sensitivity. However, because the growth of the laser intensity from the zero solution is exponentially fast, the amount of time spent between t^*, as defined in the theory, and the end of the measured delay time is always very short and does not change much at all with the frequency of the scan. By adding to the theoretical delay time this nearly constant contribution, we obtain a dependence of the delay time with an exponent somewhat larger than -1. Numerical integration of the dynamics with the

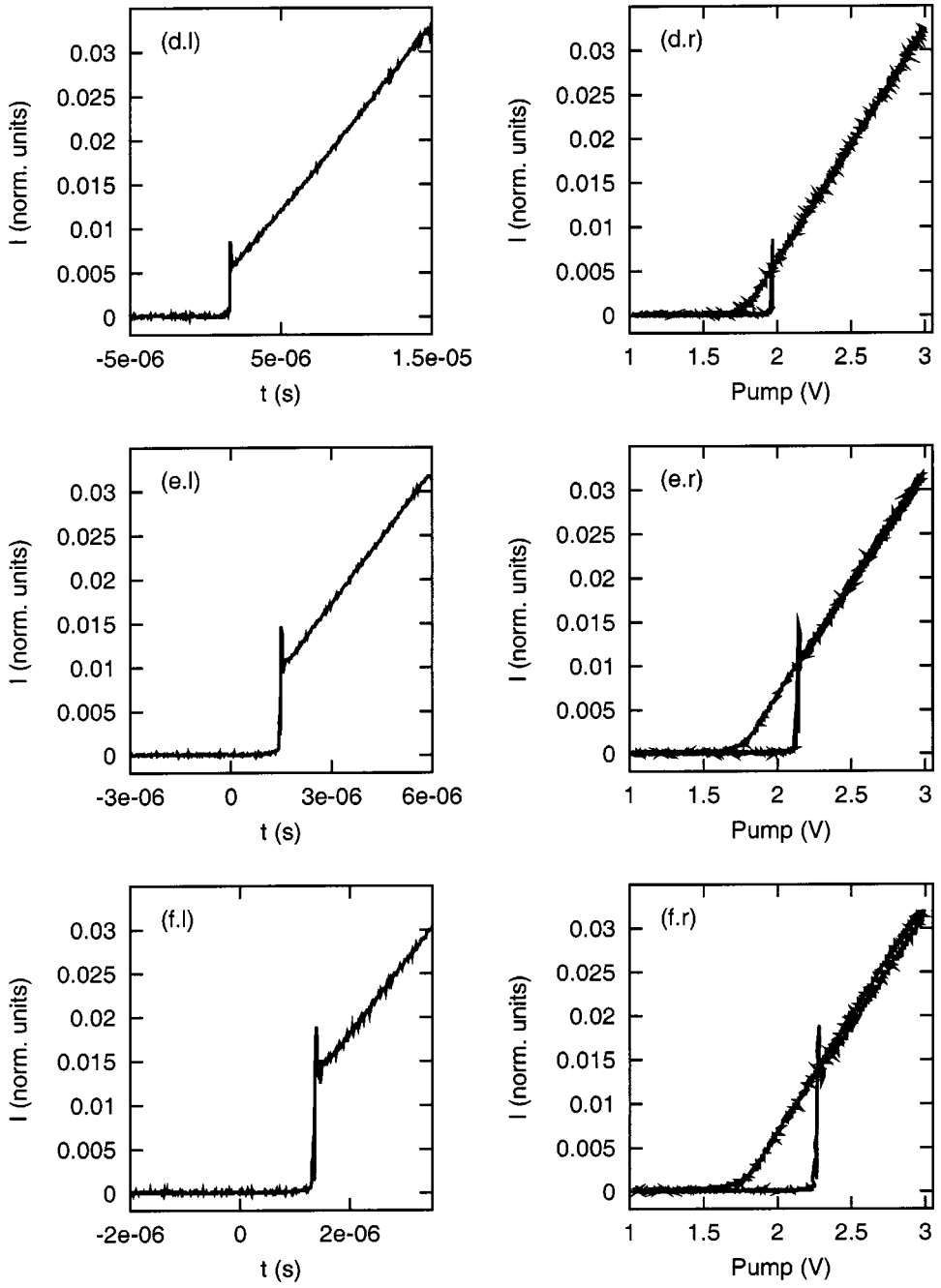

Fig. 8. (*Continued*).

time definition corresponding to that of the experiment shows, however, that the variation in the exponent amounts to only $\approx 10\%$. An additional factor that increases the exponent is the presence of noise in any experimental system. This factor has been neglected in the theoretical discussion, because we wanted to demonstrate the deterministic contribution to the delayed bifurcation. The analysis of the effects of noise is beyond the scope of this paper, but, as can be seen from Ref. 8, noise added to a dynamical system near a bifurcation point drives the system away from the unstable manifold and anticipates the jump to the other solution. In this way, the exponent x is further reduced.

A physical interpretation of the delay times can be offered to those students who have sufficient knowledge of laser physics. The laser below threshold operates with a population inversion value that is insufficient to support amplification of the optical field. While growing, the injected current (the pump) reaches the value corresponding to the point of laser emission (the threshold). This instant corresponds to $\overline{t}$, because the bifurcation has been reached by the control parameter. However, the amount of charge (number of carriers) accumulated in the semiconductor junction is not yet at the lasing level because the accumulation is achieved at a finite rate, starting from an amount of carriers below the critical one. An additional time period is needed to accumulate the number of carriers necessary to attain their threshold value; this will occur at time t^* and corresponds to reaching the dynamical bifurcation.[28]

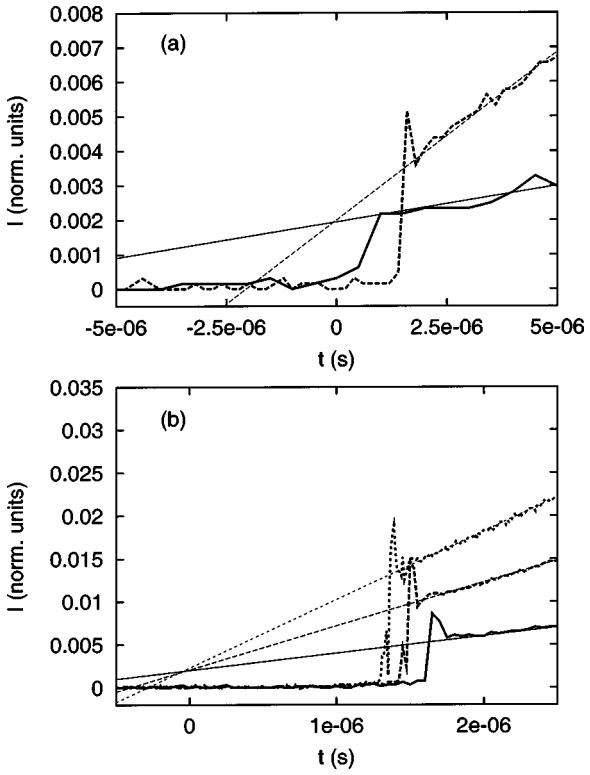

Fig. 9. (a) and (b) The variation of the delay at the bifurcation starting from the instant when the driving signal (triangle wave) crosses threshold. This choice provides the best visualization but is not the best choice for measuring the delay—see the text. In (a) the solid line represents the laser response at $f=3$ kHz, the dashed line at $f=10$ kHz. The curve at $f=1$ kHz has too low a resolution (see the text) and is not shown. The straight lines are superimposed on the linear part of the laser intensity response and are intended to guide the eye to show the expected behavior of the laser intensity in the absence of a delayed bifurcation. The shift toward positive values of the intensity of the crossing point of the straight lines (at the trigger time) is discussed in the text. (b) Same as (a) for $f=20$ kHz (solid line), $f=50$ kHz (long-dashed line), and $f=80$ kHz (short-dashed line). A reduction in the delay time for increasing frequency f is clearly visible throughout the graphs [notice the change in horizontal scale between (a) and (b)].

VII. QUESTIONS FOR STUDENTS

We offer a few questions that can be posed to students to test their degree of understanding of the physics behind the experiment and their mastery of the techniques involved.

(1) If the delay in reaching the bifurcation point grows when reducing the frequency, then why was the static threshold determined by using a very slow ramp (≈ 5 Hz in Sec. IV)?
(2) Is it possible in practice to obtain an actual measurement of the true static threshold in a real experiment? Justify your answer.
(3) Why aren't the experimental delay times measured from the point where the laser threshold is crossed?
(4) Compare the measurement of the delay time taken from the initial instant of the ramp to (a) a set threshold intensity value (any value between minimum and maximum intensity on the switch-on); (b) the mid-point of the rising intensity front (see Sec. IV); and (c) the zero-crossing of the laser intensity derivative (see Ref. 23). What are the advantages and the disadvantages of each technique?
(5) Would it be a good idea to set the trigger level in such a way as to start the trace at the point from which we want to measure the delay (the bottom point of the triangle wave)? This procedure would avoid having to use the pretrigger and the cursors (at least one of them), because we could read the time directly off the oscilloscope's scale. Comment on this procedure and explain which is the best choice.
(6) Why are Figs. 8 and 9 taken with the trigger set close to threshold for better visualization purposes?

VIII. CONCLUSION

We have shown that sweeping a control parameter across a critical point does not bypass critical slowing down. We did so by solving a simple analytic model and by conducting an experiment involving a semiconductor laser and standard lab equipment.

Although we have concentrated on the simplest aspect of the delay problem, generalizations are quite obvious. Experimentally, we could ask if t^* vanishes for large values of the sweep rate. Intuitively we would say that if b is sufficiently large, the delay time becomes equal to the response time of the system, and therefore independent of the sweep rate. This effect, that is the dependence of the response time of the system on the initial pumping value—the ''memory time''—and the dependence of the first peak amplitude on the delay time, can be easily measured in a similar experiment, but will be the subject of future work. We note that the linear equation (2) can still be solved analytically if we add a constant term (modeling an imperfection), a modulation, or noise. These generalizations are discussed in Ref. 11. Finally, whether we deal with a first- or second-order phase transition-like model does not change any of our conclusions.

Another generalization is provided by optically bistable systems.[29] In this case, the minimal equation, Eq. (1), must have a cubic nonlinearity and therefore the dependence on the sweep rate will be characterized by different exponents. The basic problem remains the same: sweeping across a critical point (here, a limit point) induces a delay generated by critical slowing down and the dynamical hysteresis is larger than the static one.

ACKNOWLEDGMENTS

The work in Brussels was supported by the Fonds National de la Recherche Scientifique and the Interuniversity Attraction Pole program of the Belgian government. We are grateful to M. Giudici for comments and discussions.

[a]Corresponding author; electronic mail: Gian-Luca.Lippi@inln.cnrs.fr
[b]Undergraduate student at the Department of Physics at the time of the work.

[1]N. B. Tufillaro and A. M. Albano, ''Chaotic dynamics of a bouncing ball,'' Am. J. Phys. **54**, 939–944 (1986); T. M. Mello and N. B. Tufillaro, ''Strange attractors of a bouncing ball,'' *ibid.* **55**, 316–320 (1987); H. T. Savage, C. Adler, S. S. Antman, and M. Melamud, ''Static and dynamic bifurcations in magnetoelastic ribbons,'' J. Appl. Phys. **61**, 3802 (1987); O. Maldonado, M. Markus, and B. Hess, ''Coexistence of three attractors and hysteresis jumps in a chaotic spinning top,'' Phys. Lett. A **144**, 153–158 (1990); S. T. Vohra, F. Bucholtz, D. M. Dagenais, and K. P. Koo, ''Direct observation of dynamic strain bifurcations and chaos in magnetostrictive amorphous ribbons,'' J. Appl. Phys. **69**, 5736–5738 (1991).
[2]S. M. Rezende, A. Azevedo, A. Cascon, and J. Koiller, ''Organizing centers of bifurcations in spin-wave instabilities,'' J. Appl. Phys. **69**, 5430–5435 (1991); D. J. Mar, L. M. Pecora, F. J. Rachford, and T. L. Carrol,

''Dynamics of transients in yttrium-iron-garnet,'' Chaos **7**, 803–809 (1997).
[3]G. Nicolis and I. Prigogine, *Self-Organization in Non-Equilibrium Systems* (Wiley, New York, 1977); J.-C. Roux, ''Experimental studies of bifurcations leading to chaos in the Belousov-Zhabotinsky reactions,'' Physica D **7**, 57–68 (1983); J. L. Hudson and O. E. Rössler, ''Chaos and complex oscillations in stirred chemical reactions,'' in *Dynamics of Nonlinear Systems*, edited by V. Hlavacek (Gordon & Breach, New York, 1985).
[4]C. Normand, Y. Pomeau, and M. G. Velarde, ''Convective instability: A physicist's approach,'' Rev. Mod. Phys. **49**, 581–624 (1977); P. Bergé, Y. Pomeau, and Ch. Vidal, *Order within Chaos* (Wiley, New York, 1984); R. P. Behringer, ''Rayleigh-Bénard convection and turbulence in liquid helium,'' Rev. Mod. Phys. **57**, 657–687 (1985).
[5]The literature is too extended to be cited here. A good overview of the problem is presented in H. Haken, ''Cooperative phenomena in systems far from thermal equilibrium and in nonphysical systems,'' Rev. Mod. Phys. **47**, 67–121 (1975), which also contains other interesting examples.
[6]H. G. Solari, M. A. Natiello, and G. B. Mindlin, *Nonlinear Dynamics* (IOP, Bristol, UK, 1996); S. H. Strogatz, *Nonlinear Dynamics and Chaos: With Applications to Physics, Biology, Chemistry and Engineering* (Perseus, Cambridge, MA, 2001).
[7]F. De Pasquale, Z. Racz, M. San Miguel, and P. Tartaglia, ''Fluctuations and limit of metastability in a periodically driven unstable system,'' Phys. Rev. B **30**, 5228–5238 (1984); R. Kapral and P. Mandel, ''Bifurcation structure of the nonautonomous quadratic map,'' Phys. Rev. A **32**, 1076–1081 (1985); G. Broggi, A. Colombo, L. A. Lugiato, and P. Mandel, ''Influence of white noise on delayed bifurcations,'' *ibid.* **33**, 3635–3637 (1986); C. Van den Broeck and P. Mandel, ''Delayed bifurcations in the presence of noise,'' Phys. Lett. A **122**, 36–38 (1987).
[8]H. Zeghlache, P. Mandel, and C. Van den Broeck, ''Influence of noise on delayed bifurcations,'' Phys. Rev. A **40**, 286–294 (1989).
[9]P. Mandel and T. Erneux, ''Laser Lorenz equations with a time-dependent parameter,'' Phys. Rev. Lett. **53**, 1818–1820 (1984); M. Lefebvre, D. Dangoisse, and P. Glorieux, ''Transients in far-infrared laser,'' Phys. Rev. A **29**, 758–767 (1984); L. Fronzoni, F. Moss, and P. V. E. McClintock, ''Swept-parameter-induced postponements and noise on the Hopf bifurcation,'' *ibid.* **36**, 1492–1494 (1987); W. Scharpf, M. Squicciarini, D. Bromley, C. Green, J. R. Tredicce, and L. M. Narducci, ''Experimental observation of a delayed bifurcation at the threshold of an argon laser,'' Opt. Commun. **63**, 344–348 (1987); M. C. Torrent and M. San Miguel, ''Stochastic-dynamics characterization of delayed laser threshold instability with swept control parameter,'' Phys. Rev. A **38**, 245–251 (1988); F. T. Arecchi, W. Gadomski, R. Meucci, and J. A. Roversi, ''Dynamics of laser buildup from quantum noise,'' *ibid.* **39**, 4004–4015 (1989); S. T. Vohra, F. Bucholtz, K. P. Koo, and D. M. Dagenais, ''Experimental observation of period-doubling suppression in the strain dynamics of a magnetostrictive ribbon,'' Phys. Rev. Lett. **66**, 212–215 (1991); D. Bromley, E. J. D'Angelo, H. Grassi, C. Mathis, and J. R. Tredicce, ''Anticipation of the switch-off and delay of the switch-on of a laser with a swept parameter,'' Opt. Commun. **99**, 65–70 (1993); S. T. Vohra, L. Fabiny, and K. Wiesenfeld, ''Observation of induced subcritical bifurcation by near-resonant perturbation,'' Phys. Rev. Lett. **72**, 1333–1336 (1994).
[10]V. N. Chizhevsky and P. Glorieux, ''Targeting unstable periodic orbits,'' Phys. Rev. E **51**, R2701–R2704 (1995); V. N. Chizhevsky, R. Corbalán, and A. N. Pisarchik, ''Attractor splitting induced by resonant perturbations,'' *ibid.* **56**, 1580–1584 (1997); K. Pyragas, ''Control of chaos via an unstable delayed feedback controller,'' Phys. Rev. Lett. **86**, 2265–2268 (2001).
[11]P. Mandel, *Theoretical Problems in Cavity Nonlinear Optics* (Cambridge U.P., New York, 1997).
[12]J. Y. Bigot, A. Daunois, and P. Mandel, ''Slowing down far from the limit points in optical bistability,'' Phys. Lett. A **123**, 123–127 (1987).
[13]The laser is a modulated visible laser diode kit, Thorlabs, Model S1031, ≈$250. A stabilized power supply can be purchased for this system from the same manufacturer. The modulating signal is coupled, from a standard function generator, directly into the laser circuit with a jack connector.
[14]High Speed Silicon Detector, 1 GHz bandwidth, Model DET 210 by Thorlabs, ≈$100.
[15]This system is no longer sold by Thorlabs and we do not know of another company selling this device. A possible replacement for this laser system could be the PMA Laser Module by Power Technology, ⟨www.powertechnology.com⟩: a laser module with built-in analogic modulation and the protections which are necessary to make it a useful student lab tool.
[16]The spontaneous emission, always present in measurable amounts in semiconductor lasers, is not considered here. In practice, no special operation is required, because the spontaneous contribution remains hidden in the trace noise of the oscilloscope when the vertical amplification is correctly chosen for the visualization of the lasing output.
[17]The logarithmic functions are natural logarithms throughout the paper.
[18]A discussion for class B lasers (Ref. 19) can be found in Sec. V.A of Ref. 20 (read the commentary to Figs. 6 and 7 in that section).
[19]J. R. Tredicce, F. T. Arecchi, G. L. Lippi, and G. P. Puccioni, ''Instabilities in lasers with an injected signal,'' J. Opt. Soc. Am. B **2**, 173–183 (1985).
[20]G. L. Lippi, L. M. Hoffer, and G. P. Puccioni, ''Noise at the turn-on of a class-B laser,'' Phys. Rev. A **56**, 2361–2372 (1997).
[21]The horizontal scale used in Fig. 6(b), chosen to display a whole period of the triangular driving, does not possess enough resolution to show the detail of the transition: an overshoot of the intensity beyond the triangular shape, with damped oscillations. This can only be seen by triggering around V^* and expanding the scale. However, one can recognize an indication of a more complex evolution from the jagged trace at the sharp front.
[22]We remark that some students, even very bright ones, will oscillate between considering the explanation obvious, when looking at the theory, and totally wrong, when sitting in front of the experiment. It may take some time and patient discussion to convince them of the fact that the experimental results truly agree with the theoretical interpretation and that their intuition and some of the experimental visualizations suggest the wrong conclusion.
[23]With digital oscilloscopes that provide the derivative of the signal, it is possible to use this feature (when the detector signal is not too noisy), to determine the ''end-time'' for the measurement of the delay. The derivative changes sign at the inflection point of the switch-up, a point that depends directly on the signal shape rather than on a threshold level set by the user. The advantage of this measurement technique, relative to the mid-height reference that we have discussed so far, is that the oscilloscope provides the end-time information without further manipulation by the user; its disadvantage is that if the signal is too noisy, then the information coming from the derivative may be difficult to exploit. In the tests we performed, however, the zero crossing of the intensity derivative always proved to be a reliable indicator.
[24]D. Bromley, E. J. D'Angelo, H. Grassi, C. Mathis, J. R. Tredicce, and S. Balle, ''Anticipation of the switch-off and delay of the switch-on of a laser with a swept parameter,'' Opt. Commun. **99**, 65–70 (1993).
[25]This upward shift in the crossing point to nonzero intensity values is related to the fact that due to the continuous sweep, the laser maintains a certain degree of memory of its state at the previous instant. As a consequence, the initial slope of the laser intensity versus time is smaller than it ought to be, and the extrapolated straight lines meet at a nonzero vertical coordinate. A discussion of the various consequences on the output intensity of a class-B laser of sweeping the pump can be found in Ref. 24. As an illustration, the flatter slope in the initial phases of lasing for growing pump values can be recognized clearly in Fig. 6(b), where the linear response regime appears to be doubled; the upsweep corresponds to the lower of the two curves. In Fig. 8 the same effect is less visible because of the scale on which the curves are plotted.
[26]G. P. Agrawal and N. K. Dutta, *Long-Wavelength Semiconductor Lasers* (Van Nostrand-Reinhold, New York, 1986).
[27]W. Scharpf, M. Squicciarini, D. Bromley, C. Green, J. R. Tredicce, and L. M. Narducci, in Ref. 9.
[28]In a semiconductor laser, as in all Class B lasers (Ref. 19), the excess population inversion necessary to initiate the optical amplification process gives rise to an additional macroscopic time delay. A discussion of this contribution, which is nonlinear and is expected to deform the distribution of points measured in Fig. 7, is beyond the scope of this paper. An understanding of its physical origin can be gained from Sec. V.A of Ref. 20.
[29]P. Jung, G. Gray, R. Roy, and P. Mandel, ''Scaling law for dynamical hysteresis,'' Phys. Rev. Lett. **65**, 1873–1876 (1990); J. Zemmouri, B. Ségard, W. Sergent, and B. Macke, ''Hesitation phenomenon in dynamical hysteresis,'' *ibid.* **70**, 1135–1138 (1993).